Comptes Rendus
Chimie
2022, 25, p. 45-52
https://doi.org/10.5802/crchim.146

Full paper / *Article*

Photodegradation of norfloxacin adsorbed on clay and carbon-clay nanomaterials: an evaluation based on antimicrobial tests

María Emilia Zelaya-Soulé [*, a], Manuel Horue [b], Rosa María Torres Sánchez [a], Guillermo Raúl Castro [b, c], Daniel Osvaldo Mártire [d], Mariela Alejandra Fernández [a] and Valeria Beatriz Arce [e]

[a] Centro de Tecnología de Recursos Minerales y Cerámica (CETMIC), (CONICET La Plata – CIC – UNLP), Cno. Parque Centenario entre 505 y 508, Gonnet, Argentina

[b] Laboratorio de Nanobiomateriales, CINDEFI, Departamento de Química, Facultad de Ciencias Exactas, Universidad Nacional de La Plata-CONICET (CCT La Plata), Calle 47 y 115, B1900AJL La Plata, Argentina

[c] Max Planck Laboratory for Structural Biology, Chemistry and Molecular Biophysics of Rosario (MPLbioR, UNR-MPIbpC). Partner Laboratory of the Max Planck Institute for Biophysical Chemistry (MPIbpC, MPG). Centro de Estudios Interdisciplinarios (CEI), Universidad Nacional de Rosario, Maipú 1065, S2000 Rosario, Santa Fe, Argentina

[d] Instituto de Investigaciones Fisicoquímicas Teóricas y Aplicadas (INIFTA), Universidad Nacional de La Plata, Diag 113 y 64, La Plata, Argentina

[e] Centro de Investigaciones Ópticas (CIOp), (CONICET La Plata – CIC – UNLP), Cno. Parque Centenario entre 505 y 508, Gonnet, Argentina

E-mails: emizelayasoule@live.com.ar, emizelayasoule@gmail.com (M. E. Zelaya-Soulé), manuelhorue@gmail.com (M. Horue), rosa.torres@gmail.com (R. M. Torres Sánchez), grcastro@gmail.com (G. R. Castro), dmartire@inifta.unlp.edu.ar (D. O. Mártire), marielafernandez0712@gmail.com (M. A. Fernández), varce@ciop.unlp.edu.ar (V. B. Arce)

Abstract. The antibiotic norfloxacin was adsorbed on clay and carbon-clay nanocomposites (MD-210 and MDac3-210-500, synthesized by hydrothermal carbonization of dextrose) but maintained its antimicrobial activity once adsorbed. To degrade it, direct (DP) and indirect (IP, with sulfate radicals) photolysis were performed. Antimicrobial activity tests were performed to evaluate the degradation generated. There were no significant differences between DP and IP for unabsorbed norfloxacin solution. The IP treatment caused a loss of antibiotic activity in all cases. For DP, the carbon samples showed better results than those of clay, evidencing the importance of oxygenated carbonaceous groups in the photolysis of norfloxacin.

* Corresponding author.

Keywords. Photolysis, Carbon-clay nanocompounds, Hybrid materials, Norfloxacin, Wastewater treatment.

Manuscript received 15th November 2021, revised 23rd December 2021, accepted 24th December 2021.

1. Introduction

Antibiotics are emerging pollutants that cause ecological imbalances and contribute to the increase of bacterial resistance in the environment, damaging the health of humans and animals. Norfloxacin (NFX) is a fluoroquinolone antibiotic that has been detected in wastewater and drinking water, and can be efficiently adsorbed on the montmorillonite clay (M) and montmorillonite-hydrothermal carbon nanocompounds (named MD-210 and MDac3-210-500) [1,2]. According to Zelaya Soulé *et al.* [1], hydrothermal synthesis emerges as an environmentally friendly and low-cost alternative to conventional carbon synthesis, it is carried out at a low temperature (210 °C) and does not involve strong solvents. The products developed with dextrose as the carbon source, as MD-210 and MDac3-210-500, presented a large amount of oxygenated groups on their surface, with double bonds and aromatic groups, which intervened in the adsorption process of NFX [2,3].

Despite M being reported to have the highest NFX adsorption capacity at pH = 7, the nanocompound MDac3-210-500 resulted in a better adsorption of NFX when successive adsorptions were performed [1]. This result along with the fact that M cannot be used in filters due to its high swelling capacity favors MDac3-210-500 as a possible column filler. The previous studies of NFX adsorption in batch and also in continuous systems (columns with MDac3-210-500 as adsorbent material), constituted a prior step to encourage the construction of a domestic filter system [2]. The extra goal, that the NFX adsorbed on M, MD-210, and MDac3-210-500 samples did not desorb during four adsorption–desorption cycles performed in water at pH = 7 [1], is no less important. However, due to the danger of the presence of NFX in the filtering system, when used in drinking water treatment, it is necessary to evaluate if the retained NFX maintains its antimicrobial activity, also to assess its correct final disposal and/or recycle the solid.

Photodegradation (or photolysis) is the decomposition of a compound caused by the action of natural or artificial light, in the UV-VIS-IR zones. Direct photolysis involves the transformation of a chemical resulting from the direct absorption of a photon. Indirect photolysis (IP) requires that other components of the medium (known as photosensitizers) absorb the light and generate reactive species, such as hydroxyl and nitrate radicals, that can interact with the compound of interest [4]. The sulfate radical (SO_4^*) exhibits broad applications in chemical, biomedical, and environmental sciences, due to its redox potential of ca. 2.6 V, similar to the hydroxyl radical [5]. Sulfate radicals-based advanced oxidation processes are promising technologies for soil and groundwater remediation. In particular, the generation of sulfate radicals, achieved by photolysis of peroxydisulfate ($S_2O_8^{2-}$), has been shown to degrade NFX [6,7]. In the present work, this treatment is employed as the indirect photolysis method to achieve the degradation of NFX.

The large number of oxygenated groups, double bonds, and aromatic groups of the hydrothermal carbons [2,3] that can absorb light, raises the possibility that they could favor the indirect photolysis of adsorbed pollutants. In this sense, this work hypothesizes that these organic groups in carbon-clay nanocomposites (MD-210, and MDac3-210-500) could benefit the photodegradation of adsorbed NFX, when compared to NFX adsorbed on M. This hypothesis arose as a consequence of two observations:

(1) in natural environments there is an important effect of the matrix on the substance to be degraded since photolysis usually occurs because humic substances, microorganisms or algae contain sunlight-absorbing chromophores [4,8]. It has been noticed, for example, that the presence of photosynthetic microorganisms in soil and of reactive oxygen species in water, favor the photolysis of pesticides [4,9].

(2) When a photocatalyst made by ultrasound-assisted hydrothermal fabrication of AgI/$MFeO_3$/g-C_3N_4 (M = Y, Gd, La) with a nanosheet–sphere–sheet structure was used, the release of electrons and reactive oxygen species ($\cdot O_2^-$, h^+ and $\cdot OH$) improved the NFX degradation [10].

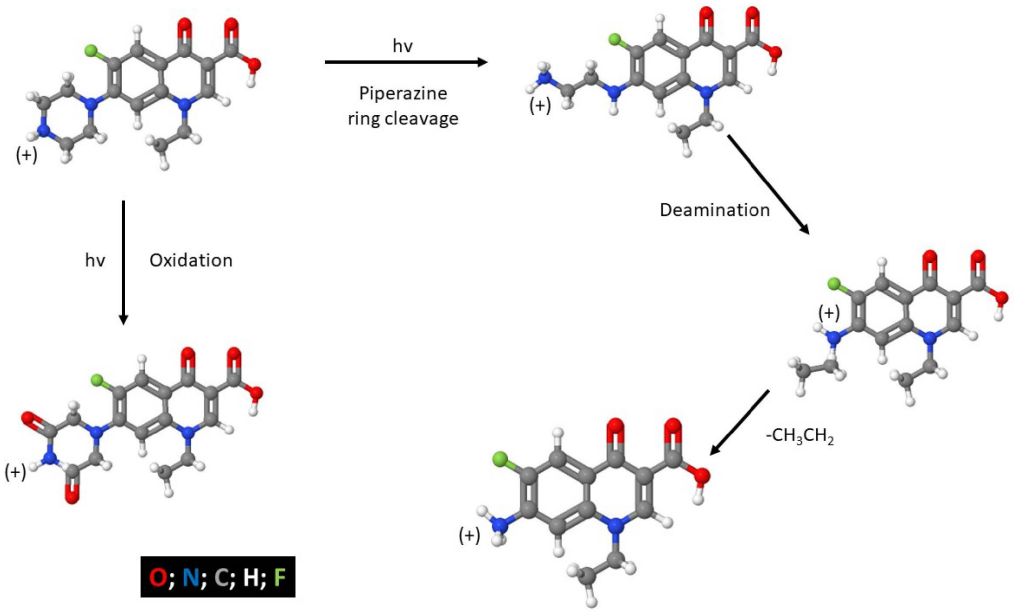

Figure 1. Degradation products of NFX at pH = 7.

It is critical to keep in mind that photolysis does not necessarily mean mineralization and might lead to intermediate products that can be even more toxic than the parent compound. This makes it necessary to study the nature of the reaction products if a total degradation is not reached [4]. Photodegradation of NFX produces at least five identified products (Figure 1), whose stability depends on the medium pH [8,11]. Besides, it has been observed that the photodegradation of NFX (at λ = 274 nm lamps) is more effective in a pH range of 6–10, due to the occurrence of a light-sensitive zwitterionic form of NFX [11].

Since the primary objective of degrading the antibiotic is to remove its antimicrobial activity, thus reducing its associated risks, antimicrobial tests against *Escherichia coli* were carried out to compare the antimicrobial activity of NFX retained on the solids before and after photodegradation. A similar methodology was previously used to evaluate the remaining antibacterial capacity after tetracycline photocatalysis degradation with TiO_2 [12]. Although this procedure does not ensure the complete degradation of the compound, it can assess whether pure NFX or its (more) active metabolites decrease their antimicrobial activity after irradiation.

2. Experimental section

2.1. *Materials*

The raw montmorillonite (M) was supplied by Castiglioni Pes and Cia. (*Río Negro* province, Argentina) and used without purification [13]. The MD-210 and MDac3-210-500 materials were synthesized as indicated in previous work [2]. Briefly, both samples were obtained by hydrothermal carbonization at 210 °C for 24 h, with dextrose (D) as carbon source. The MDac3-210-500 sample was achieved from an M+D suspension with 0.50 V/V of H_3PO_4/distilled water; followed by the hydrothermal treatment, and additional post-activation at 500 °C for 1 h in an inert atmosphere. The specific surface values, measured with N_2 as adsorbate, were 65.5 m^2/g, 1.2 m^2/g, and 131.6 m^2/g for M, MD-210 and MDac3-210-500, respectively [2].

NFX (MW = 319.33 g/mol, solubility in water 0.39 g/L, and isoelectric point = pH 7.4) was purchased from Parafarm. The sodium peroxydisulfate ($Na_2S_2O_8$) was provided by Merck.

Deionized water (>18 MW·cm^{-1}, <20 ppb of organic carbon) was obtained with a Millipore Co. (Billerica, Ma, USA) water purification system.

2.2. *Adsorption and photodegradation experiments*

The NFX adsorption experiments at pH = 7.0 ± 0.5 were performed previously and rendered ca. 74% of NFX adsorption on M and MD-210, and 30% on MDac3-210-500 [1,2,14]. The photodegradation of NFX adsorbed on M, MD-210 and MDc3-210-500 was also studied at pH = 7.0 ± 0.5. The pH value was chosen because it is close to the pH of drinking water, and the NFX is present in a zwitterionic form, allowing an optimal photodegradation [11].

To monitor the possible desorption of the antibiotic because of the light treatment, the NFX concentration in the suspensions after irradiation was quantified by HPLC. In addition, the concentration of the free NFX solution was also measured after direct and indirect irradiation. The column employed was a Shimadzu C18 (4.6 mm × 250 mm, 4.6 μm), at λ = 278 nm, phosphate buffer:water rate of 25:75 at pH = 3.0 ± 0.5, 0.8 mL/min, volume injection = 10 μL and retention time = 3.7 min (R^2 = 0.999 for the calibration curve).

Direct photodegradation (DP)

100 mg of each adsorbent material was mixed with 100 mL of 0.65 mM NFX at pH = 7.0 ± 0.5, 25 °C, and stirred for 24 h at 700 rpm. The NFX concentration in the resulting solids was 0.56 mmol/g for M and MD-210, and 0.21 mmol/g for MDac3-210-500. To normalize the photodegradation assays, a solid mass with 2.34 mg of NFX adsorbed was used in all cases (this corresponded to 13 mg of M and MD-210, and 35 mg of MDac3-210-500). The solids were suspended in 70 mL of Mili Q water and irradiated in a Rayonet RPR-100 reactor equipped with eight lamps (λ = 254 nm). The free 0.65 mM NFX solution was also irradiated and used as a control. To evaluate the photodegradation, aliquots of the suspensions were taken during the experiments at 0, 1, 2, and 3 h, and their absorption spectra were immediately measured with a UV–VIS spectrophotometer (T90+PG). The absence of significant changes in two consecutive spectra was used to decide the end of irradiation.

Indirect photodegradation (IP)

0.4 or 0.1 M $Na_2S_2O_8$ as additive was incorporated in M suspensions, and only 0.1 M to the suspensions of the carbon-clay nanocomposites. The initial NFX solution was used as a control sample. The irradiation was performed for 20 min with eight lamps of λ = 300 nm. A different λ was used in the IP, compared to that used in the DP assays, because at λ = 254 nm both IP and DP effects could occur, and the intention was to evaluate the effects separately. Due to the overlap between $Na_2S_2O_8$ and NFX absorption spectra (Figure S1, in supporting information), only the antimicrobial test was used in the IP experiments to evaluate the success of the NFX photodegradation.

2.3. *Antimicrobial tests*

The potential changes in the NFX antimicrobial activity after the DP and IP treatments were evaluated against *Escherichia coli*. Suspensions of 0.5 mg/mL of the adsorbents were placed in the plates, and the antimicrobial activity was compared to those of the following control samples: 0.65 mM of NFX solution (NFX), 0.65 mM solution of NFX with the DP treatment (NFX-DP) and 0.65 mM solution of NFX with the IP treatment (NFX-IP).

The agar diffusion method was employed to assay the antimicrobial activity. *Escherichia coli* (ATCC 25922) was precultured in nutrient broth before starting the tests and incubated at 37 °C for 24 h. After that period, a new bacterial inoculum containing 1.5 × 10^8 UFC/mL was seeded in Petri dishes containing Mueller Hinton agar. Then, sterile disks were placed over the plates to contain and limit the dispersions of the samples and solutions (of which 50 μl were cultivated). They were left incubating at 37 °C for 24 h until the patina development and the inhibition halos were measured. The antimicrobial activity of each sample was evaluated by measuring the diameter of the halo, performed with the free software ImageJ V. 1.46r [15]. All experiments were done in duplicate.

3. Results and discussion

The UV–VIS spectra of the 0.65 mM NFX solution which was diluted ten times, as well as the DP samples, are shown in Figure 2. As was indicated in the experimental section (Section 2.2), this measurement was used to choose the time to finish the irradiation.

The NFX initial solution concentration after irradiation was lower than the detection limit of the HPLC equipment utilized, indicating that the antibiotic was almost completely degraded.

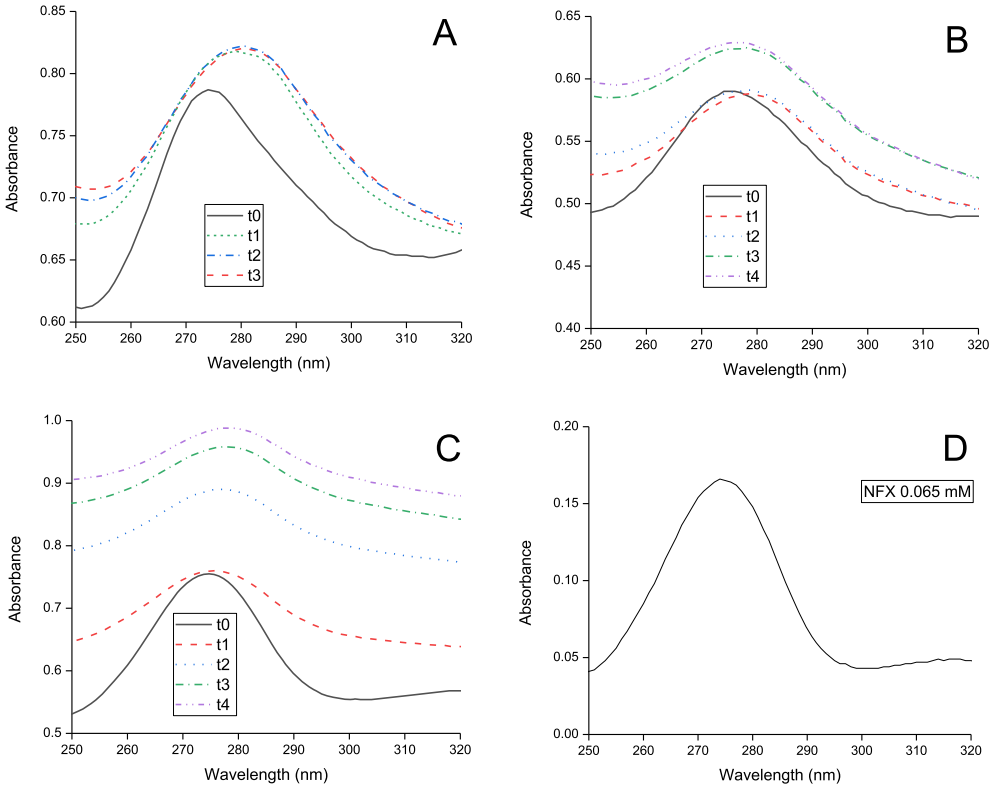

Figure 2. UV–VIS spectra after direct photolysis, at the indicated time (in hours), of NFX adsorbed in: (A) M, (B) MD-210, (C) MDac3-210-500, and (D) the initial concentration of NFX with a 1/10 dilution.

Initially (named t0) the NFX bands were detected in all samples, although, probably due to the presence of the solid (Figure 2A, B, and C)—the NFX did not desorb from samples in deionized water at pH = 7 [1]—, the baseline of the spectra changed in the samples with adsorbent material in comparison to the spectrum of the NFX initial solution (Figure 2D).

During the DP treatment, the NFX absorption bands underwent shape modifications assigned to NFX photodegradation, that could release intermediate products that absorbs in the wavelengths shown (Figure 2). The absence of NFX desorption during the photodegradation treatment was evidenced by obtaining a negligible NFX concentration in the supernatants of the NFX adsorbed on the different materials. According to the criteria adopted to end the experiment, the M+NFX sample was irradiated for 3 h (t3), and the MD-210+NFX and MDac3-210-500+NFX samples, for 4 h (t4).

To evaluate the variation in NFX during photodegradation, the comparison of shape and intensity of bands was made in the UV spectrum for each sample at different times (in each figure, the spectrum at t0 was compared to those at other times viz., t1, t2, t3 and t4). No quantitative comparison was performed between spectra of different samples, therefore Figures 2A, B, and C do not have the same scale on the ordinate axis. In this sense, the scale of each figure was chosen to easily show the changes that were taking place. The changes in the spectra measured on the MD-210 and MDac3-210-500 samples (Figure 2B and C) from t0 and t4, were more pronounced than that observed for NFX adsorbed on M (Figure 2A) from t0 to t3. Since the highest modifications of the spectra between the initial and final times occurred for the carbon-clay compounds, the degradation of NFX in these samples could be at a more advanced degree than in M. The spectral analysis provided relevant qualitative information, showing that the NFX molecule was changing when interacting with light. This encouraged antimicrobial testing, which will be discussed below.

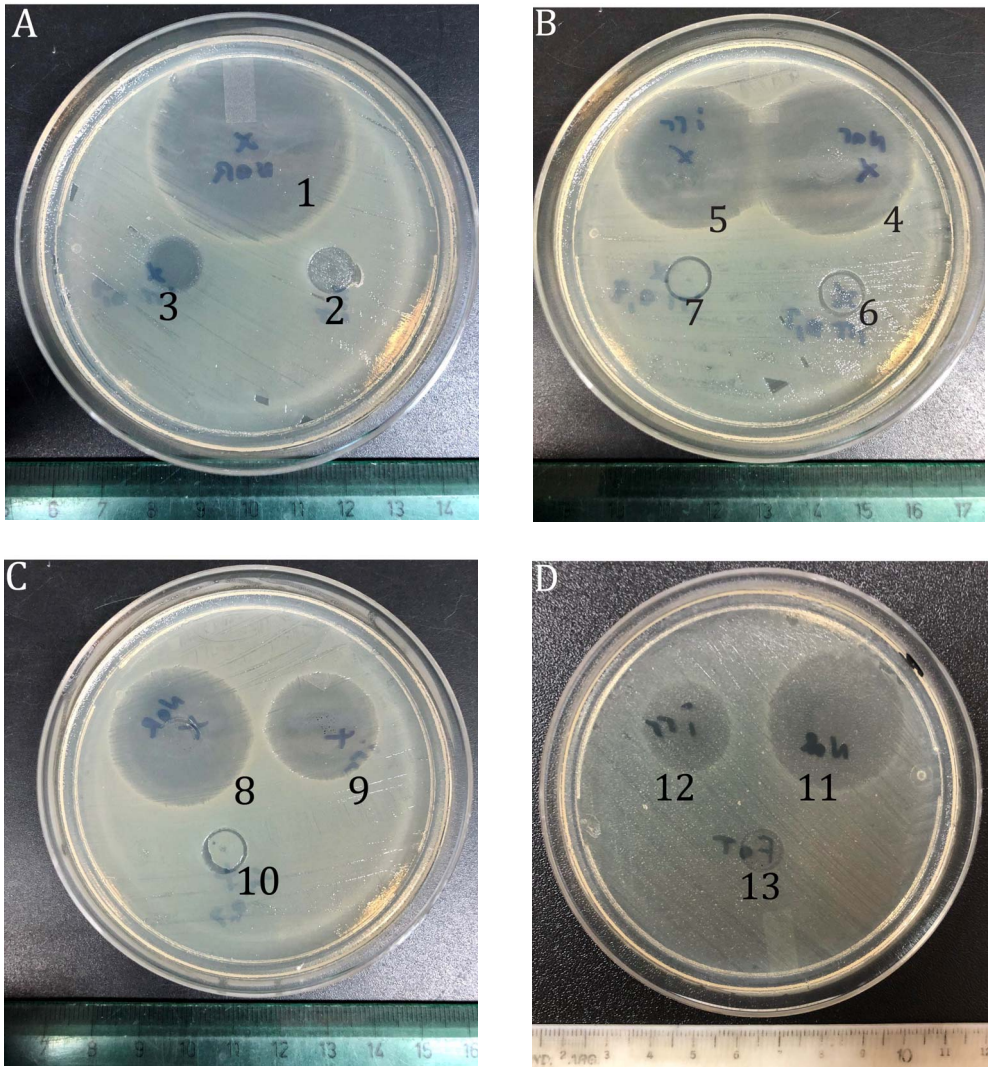

Figure 3. Agar diffusion assay against *E. coli*. Each plate contains an adsorbent material with different applied treatments. The numbers correspond to samples listed in Table 1.

The plates of inhibition halos, measured by agar diffusion assay against *E. coli*, are depicted in Figure 3, and halo diameters are summarized in Table 1.

M and MD-210 samples adsorbed more NFX per gram than MDac3-210-500, whereas in the antimicrobial tests the concentration of adsorbent was always 0.5 mg/mL (so, it has the lowest NFX amount per gram of adsorbent in the MDac3-210-500 plate). However, the three materials yielded similar diameters of halos (Table 1), indicating that MDac3-210-500 preserves more the adsorbed antibiotic activity than M and MD-210. The characterization performed in previous works revealed that the M and carbon-clay nanocompounds presented negatively charged electrical surfaces, and that the nanocompounds were more hydrophilic than M [1,2]. Thus, two predominant interaction types of NFX with the samples at the adsorption pH (pH = 7.0 ± 0.5) are possible: (a) electrostatic attraction of the positive amine group of NFX with the negative carbon-clay compounds or the negative M surface (internal and external), and (b) π–π donor–acceptor electron interaction between the F atom of the benzene group of the NFX and the

Table 1. Diameters of inhibition halos measured by agar diffusion assay against *E. coli*

Samples	Diameter (mm)
(1) NFX	36.0 ± 0.2
(2) NFX-DP	9.00 ± 0.05
(3) NFX-IP	10 ± 3
(4) M+NFX	31 ± 2
(5) M+NFX-DP	29.0 ± 0.2
(6) M+NFX-IP	N.O.
(7) M+NFX-IP 0.4	N.O.
(8) MD-210+NFX	28.5 ± 0.7
(9) MD-210+NFX-DP	23 ± 2
(10) MD-210+NFX-IP	N.O.
(11) MDac3-210-500+NFX	31.21 ± 0.05
(12) MDac3-210-500+NFX-DP	20.4 ±0.6
(13) MDac3-210-500+NFX-IP	N.O.

"N.O." was placed when no inhibition halo was observed. For the "IP" treatment the additive concentration was 0.1 M, except for sample M+NFX-IP 0.4, where it was 0.4 M.

double bond or aromatic carbon groups [16]. For MDac3-210-200, the NFX adsorption occurs on the external surface and mostly by π–π donor–acceptor electron interaction with the external groups, due to the interlayer space wreckage by the acid treatment executed to improve the specific surface of the sample. In contrast, in M and MD-210 most of the NFX adsorption takes place in the interlayer space by electrostatic attraction. Consequently, the external surface interaction of MDac3-210-500 with the NFX molecule seems to favor the availability of the active part of the antibiotic molecule against *E. coli*.

When DP was performed on the free NFX (sample 2 in Table 1), the diameter of the inhibition halo decreases 27 mm compared to the NFX without irradiation (sample 1), evidencing a significant decrease in the antimicrobial activity of NFX. The halo diameter of the M+NFX sample did not change substantially after the DP treatment, correlated with the slight spectral variation observed in Figure 2A. Among the NFX adsorbed on carbon-clay samples, the DP treatment produced the highest loss of the antibiotic activity for NFX adsorbed on MDac3-210-500 (with a decrease of 9 mm between sample 12 and 11), in which NFX is adsorbed at the external surface. For MD-210 there was a reduction of 5 mm, and the NFX adsorption occurred mainly in the interlayer space.

The observations mentioned above also agree with the working hypothesis: the double bonds, oxygenated and aromatic functional groups of carbon facilitate the DP of the retained NFX. Future radical-quenching experiments will be useful to reveal the mechanism of degradation in these materials. In addition, when NFX is on the external surface (as in the MDac3-210-500 sample) the interaction with the light was improved, compared to its location in the interlayer space (M and MD-210 samples). However, although the NFX activity after DP slightly decreased, the antibiotic remained active. Thus, an IP strategy was proved to enhance the destruction of the NFX-active form.

When $Na_2S_2O_8$ was used (Table 1 and Figure 3) the diameter of the inhibition halo (see NFX-IP) was not significantly different from the NFX-DP. This result indicates that when NFX is in its free form (not adsorbed), the additive does not enhance its photodegradation. Besides, the NFX-IP adsorbed on the three adsorbent materials (samples 6, 7, 10, and 13 in Table 1) did not show inhibition halo: a higher degree of degradation was achieved in these cases, compared to the NFX-free IP (sample 3).

For the M sample (number 6 of Figure 3) neither the 0.1 M nor 0.4 M of $Na_2S_2O_8$ showed inhibition halo, indicating that IP degraded the NFX adsorbed on M, or at least its active form. Because of this result, only 0.1 M $Na_2S_2O_8$ was employed with the other adsorbent materials. Similarly, the MD-210+NFX-IP and MDac3-210-500+NFX-IP (numbers 10 and 13 in Table 1 and Figure 3) did not display inhibition halo. The additive contributes to the degradation of NFX, to such an extent that the amount of remaining antibiotic does not have sufficient bactericidal capacity to develop a halo.

4. Conclusion

NFX adsorbed on the clay and carbon-clay nanocomposites maintained its antimicrobial activity, which could promote bacterial resistance and harm human and animal health. Due to the interaction of NFX exclusively with the external surface of the MDac3-210-500 sample, the antibiotic functional groups could be

more exposed to microorganisms and thus preserve more antimicrobial activity, compared to the M and MD-210 samples.

The direct photodegradation of the antibiotic was partially successful for free NFX and the NFX adsorbed on carbon-clay nanocomposites. However, the NFX activity decreased but did not disappear completely. The changes observed between the average diameters before and after irradiation could be assigned to the double bonds, oxygenated and aromatic groups of carbon, which could favor the interaction with the light. The sample with the lowest diameter of inhibition halo was MDac3-210-500, which could be related to the external surface interaction between this sample and NFX, mentioned above. The NFX adsorbed on M did not suffer a significant degradation after the DP treatment.

When an indirect photodegradation pathway was used, the inhibition halo of free NFX (NFX-IP) was like that of NFX-DP, showing that when NFX is not adsorbed, it is not worth adding the additive. The NFX-IP adsorbed on the three materials failed to inhibit the growth of microorganisms on the plates, suggesting the success in the destruction of the active NFX.

Additionally, the high antimicrobial activity of NFX adsorbed on MDac3-210-500, found in this work, raises the possibility of its uses for the development of drug-controlled release devices, helping to maintain the threshold dose of NFX for a longer time.

Conflicts of interest

The authors state that they have no known competitive financial interests or personal relationships that could have affected this work.

Acknowledgments

MEZ-S and MH acknowledge the National Council of Scientific and Technological Research (CONICET) fellowships. MAF, GC, and RMTS acknowledge the CONICET. DOM and VBA are research members of CIC, Buenos Aires, Argentina. The present work was partially supported by grants of Universidad Nacional de La Plata (11/X815) and ANCyT (PICT2017-0359) to GRC.

This work was supported by the Argentine Ministry of Science (ANPCyT—PICT-2018-03451).

Supplementary data

Supporting information for this article is available on the journal's website under https://doi.org/10.5802/crchim.146 or from the author.

References

[1] M. E. Zelaya Soulé, F. Barraqué, F. M. Flores, R. M. Torres Sánchez, M. A. Fernández, *Adsorption*, 2019, **25**, 1361-1373.

[2] M. E. Zelaya Soulé, F. M. Flores, R. M. Torres Sánchez, M. A. Fernández, *J. Environ. Sci. Heal. Part A*, 2020, **56**, 113-122.

[3] M. E. Zelaya Soulé, M. A. Fernández, M. L. Montes, F. Suárez-García, R. M. Torres Sánchez, J. M. D. Tascón, *Colloids Surf. A Physicochem. Eng. Asp.*, 2020, **586**, article no. 124192.

[4] L. Sánchez Prado, "Estudio de la fotodegradación de compuestos orgánicos mediante microextracción en fase sólida, cromatografía de gases y espectrometría de masas", PhD Thesis, Universidad de Santiago de Compostela, Spain, 2007.

[5] H. Y. Gao, C. H. Huang, L. Mao, B. Shao, J. Shao, Z. Y. Yan, M. Tang, B. Z. Zhu, *Environ. Sci. Technol.*, 2020, **54**, 14046-14056.

[6] M. L. Dell'Arciprete, C. J. Cobos, D. O. Mártire, J. P. Furlong, M. C. Gonzalez, *New J. Chem.*, 2011, **35**, 672-680.

[7] C. Jiang, Y. Ji, Y. Shi, J. Chen, T. Cai, *Water Res.*, 2016, **106**, 507-517.

[8] S. Babić, M. Periša, I. Škorić, *Chemosphere*, 2013, **91**, 1635-1642.

[9] J. P. Escalada, V. B. Arce, G. V. Porcal, M. A. Biasutti, S. Criado, N. A. García, D. O. Mártire, *Water Res.*, 2014, **50**, 229-236.

[10] J. Zhang, Z. Zhu, J. Jiang, H. Li, *Catalysts*, 2020, **4**, article no. 373.

[11] I. Ahmad, R. Bano, S. G. Musharraf, M. A. Sheraz, S. Ahmed, H. Tahir, Q. Ul Arfeen, M. S. Bhatti, Z. Shad, S. F. Hussain, *J. Photochem. Photobiol. A Chem.*, 2015, **302**, 1-10.

[12] C. Reyes, J. Fernández, J. Freer, M. A. Mondaca, C. Zaror, S. Malato, H. D. Mansilla, *J. Photochem. Photobiol. A Chem.*, 2006, **184**, 141-146.

[13] A. M. Fernández Solarte, J. Villarroel-Rocha, C. F. Morantes, M. L. Montes, K. Sapag, G. Curutchet, R. M. Torres Sánchez, *C. R. Chim.*, 2019, **22**, 142-153.

[14] M. E. Zelaya Soulé, "Obtención de nanocompuestos montmorillonita/carbono (a partir de hidratos de carbono) para remoción de contaminantes emergentes presentes en aguas residuales", PhD Thesis, Universidad Tecnológica Nacional, Argentina, 2020.

[15] W. S. Rasband, "ImageJ", 1997, US National Institutes of Health, Bethesda, MD.

[16] Z. Wang, B. Pan, B. Xing, *Environ. Sci. Technol.*, 2010, **44**, 978-984.